Amorphous-amorphous transitions in silica glass. I. Reversible transitions and thermomechanical anomalies

Liping Huang* and John Kieffer
Department of Materials Science and Engineering, University of Michigan, Ann Arbor, Michigan 48109-2136, USA
(Received 2 September 2003; revised manuscript received 5 January 2004; published 16 June 2004)

Amorphous-amorphous transitions in silica glass under a variety of thermomechanical conditions are studied with molecular-dynamics simulations using a charge-transfer three-body potential model. The polyamorphic transitions can be reversible or irreversible depending on the combination of pressure and temperature at which the transitions take place. Anomalous thermomechanical behaviors of silica glass, such as an increase of the mechanical moduli upon expansion as a result of tensile deformation or thermal expansion, are well reproduced in our simulations. In part I, we show these anomalies are due to reversible structural transitions, which activate similar structural modes of displacement as in the α-to-β phase transformations in cristobalite silica. The emergence of dynamic instabilities is observed in conjunction with these reversible structural changes, characterizing them as transitions rather than gradual deformations. The polyamorphic transitions are gradual and localized in silica glass in contrast to the instantaneous and extended character of polymorphic transformation in crystals. The mechanism of the irreversible transitions, the negative thermal expansion of silica glass under pressure, as well as the effect of pressure and temperature on the permanent densification of silica glass and the nature of the newly discovered amorphous phases are discussed in part II.

DOI: 10.1103/PhysRevB.69.224203 PACS number(s): 61.43.Fs, 62.50.+p, 64.70.−p, 02.70.Ns

I. INTRODUCTION

Silica glass, one of the most widely and well-studied materials both theoretically and experimentally, has drawn much attention for decades not only as an archetype of an amorphous material, but also because of its anomalous thermomechanical properties. Experiments have shown that in some temperature regimes it exhibits negative thermal expansion,[1] the elastic moduli of silica glass increase with increasing temperature,[2–4] and the bulk modulus passes through a minimum upon compression at $\sim 2-3$ GPa.[5–9] Furthermore, this material can undergo irreversible densification under pressure.[10–17] Models proposed to explain these phenomena are in one way or another based on the assumption that two or more energetically distinct amorphous states coexist in proportions that vary with pressure and temperature,[9,18] but for the most part little detail is provided as to the structural entities that constitute these states and the atomic-scale mechanisms that underlie the structural transitions between the states. In recent years, considerable effort has been devoted to studying the amorphous-amorphous transitions and densification of silica glass under various mechanical and thermal conditions.[11–17,19–30] Yet to date the exact nature of the structural transitions that the glass undergoes, as well as the nature of the newly discovered amorphous phases, have not been determined due to the scarcity of structural probes for characterizing the materials under the extreme conditions at which the structural transitions take place. Changes affecting the near-range order, such as a possible increase of Si coordination from 4 to 6 can relatively easily be evidenced. However, when it comes to identifying topological changes that affect the intermediate-range order, progress is impeded by the prevailing difficulties in characterizing amorphous structures, especially considering the limited spatial and temporal resolution of current experimental techniques. In this context, molecular-dynamics (MD) simulations can complement experiments.

As the archetypical glass-forming oxide, silica has been the subject of a number of simulation studies aimed at elucidating different structural aspects, including the effects of pressure on the near-range and intermediate-range structural order.[21,24,26,27] Simulations based on the simpler central-force potentials, especially the more recent approaches that assume partial charges for individual species are quite successful in reproducing experimentally determined structural characteristics, while three-body potentials, which take directional forces into account, yield more accurate vibrational properties. The absence of directional forces tends to provide for higher atomic mobility and therefore a more relaxed glass structure. For the same reason central-force models predict a premature transition between low- and higher-coordinated structural units upon compression. While coordination changes at low pressures observed in simulations have been proposed as the mechanism for the permanent densification of amorphous silica, there exists no experimental evidence for this process. Hence, the structural developments upon densification of silica glass may not be fully explained. Moreover, the origin of the anomalous thermomechanical behaviors in this material has so far not been identified. This aspect is the focus of the present paper. For the investigation of this phenomenon we used MD simulations based on an interaction model that includes dynamic charge transfer, the advantages of which are outlined in the following section.

II. DETAILS OF SIMULATIONS

A. Potential model

In this paper we study silica glass based on molecular-dynamics simulations using a charge-transfer three-body po-

tential model. In this interaction potential, the directional character of the covalent bonding in SiO_2 is modeled by means of three-body terms that constrain both the Si-O-Si and O-Si-O angles. In addition, a charge-transfer term controls the degree of charge polarization in a covalent bond, as well as the amount of charge transferred between atoms upon rupture or formation of such a bond. Using this potential, we can simulate the α-to-β transformations in various crystalline forms of silica without need to change potential parameters. Details about the potential formula and parameters can be found in our earlier paper.[31]

The use of three-body interactions for this study is indicated by the need to reproduce the effect of a lone pair of electrons on the oxygen, which causes the Si-O-Si bond to deviate from a linear configuration. (The two Si-O bonds joining at the same oxygen form an angle of approximately 150°.) The bond polarization is described by a charge-transfer function, which not only controls the balance between covalent and ionic character of atomic interactions, but also determines the way the nominal charge on each atom depends on its immediate environment. In particular, this interaction model accounts for charge redistributions that occur upon rupture and formation of bonds, and in general provides for greater reactivity of species. For the current study, our charge-transfer three-body potential was parametrized for fourfold coordinated Si. This assures us of an accurate model up to the pressure at which the Si coordination changes from 4 to 6, which is shown to be above 20 GPa in experiments.[14,28,32]

B. Preparation of silica glass

MD simulations of silica glass were carried out for 648-particle (216 Si and 432 O) and 3000-particle (1000 Si and 2000 O) systems with periodic boundary conditions. No system size effects in excess of statistical errors could be detected between the two. The room-temperature zero-pressure glass was obtained by heating and melting cristobalite silica and subsequently cooling the liquid silica at a rate not exceeding 0.25 K/ps. Equilibrating the silica melt at different maximum temperatures and for various amounts of time did not affect the behavior of the glass. The equations of motion were integrated using the fifth order Gear predictor-corrector algorithm[33] with a time step of 2 fs. As seen in Fig. 1, the initial silica glass has a density of 2.24 g/cm^3 at 300 K, a positive thermal expansion in the low-temperature range, and a density maximum at higher temperature. All of these features are in good agreement in experiments and other simulations.[34]

C. Determination of structure and properties

The elastic properties of silica glass were determined at ambient pressure from 300 K to 2000 K at 50 K intervals, using a heating rate of 5 K/ps followed by 20 ps equilibration at each point. Conversely, the hydrostatic compression-decompression was carried out on equilibrated structures at 500 K, 1000 K, and 1500 K from −20 GPa to 20 GPa at 1 GPa intervals, using a compression rate of 0.5 GPa/ps. Temperature ramping was achieved by velocity scaling and the density adjusts according to the Anderson constant-pressure algorithm.[35] The bulk modulus of silica glass was calculated directly from the equation of state according to $B=\rho(dP/d\rho)$.

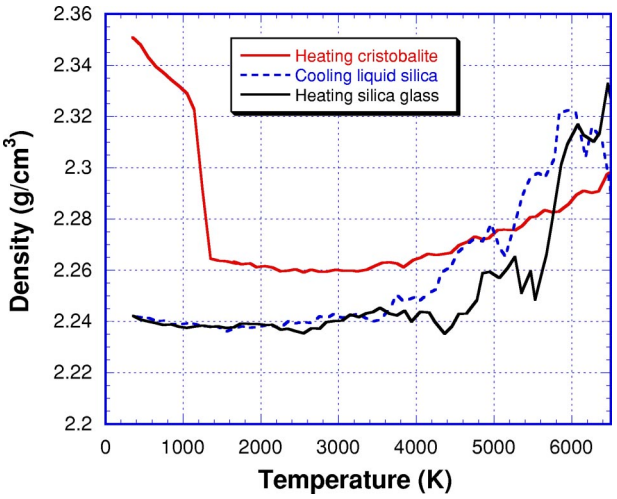

FIG. 1. Thermal cycle for the preparation of simulated silica glass: heating cristobalite to liquid silica and quenching to room temperature. Subsequent heating reveals the expected thermal properties of silica glass under ambient pressure.

The structure factors as well as the short-range order of silica glass were calculated after equilibration at each state point using standard formalisms of statistical mechanics. Ring statistics, based on shortest-path analysis[36–38] was employed to characterize the structure of the silica glass network on the intermediate length scales. To analyze the modes of structural reorganization in silica glass we monitored the order parameter that we identified in a previous study as most indicative of the α-to-β cristobalite phase transformations in crystalline silica.[31] This order parameter is given by the orientation of the normal to the plane formed by the two Si-O bonds in each Si-O-Si bridge and will be explained in detail below. The dynamical properties of the silica glass were based on the vibrational density of states (VDOS), as determined from the eigenvalues of the dynamical matrix $(m_i m_j)^{1/2}\partial^2\Phi(\mathbf{R})/\partial\mathbf{R}_{i\alpha}\partial\mathbf{R}_{j\beta}$, where i and j are atom indices, α and β are the Cartesian components.

III. RESULTS AND DISCUSSION

A. Response to temperature changes

As seen in Fig. 2(a), the initial bulk modulus of silica glass at 300 K is 49 GPa and is higher than the experimental 37 GPa as shown in Fig. 2(b),[2] but lower than 82 GPa from a recent electronic structure calculations of silica glass under pressure.[39] The anomalous temperature dependence of the elastic properties of the glass, e.g., the increase of the bulk modulus with increasing temperature, is indeed reproduced in our simulations, albeit the rate of increase of the modulus with temperature is about four times smaller than that in experiments. This can be attributed to the enormous quench rates and the ensuing high fictive temperatures of the simulated glasses. From the positive temperature dependence of

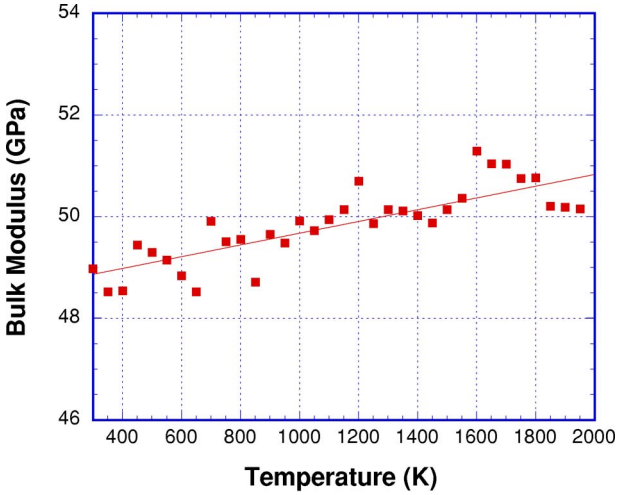

(a)

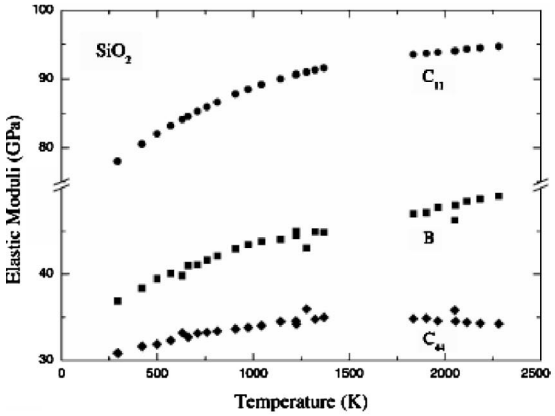

(b)

FIG. 2. Elastic moduli of silica glass versus temperature at ambient pressure: (a) bulk modulus from our MD simulations; (b) elastic constants C_{11}, C_{44} and bulk modulus from experiments (Ref. 2).

the elastic modulus we know that at high temperatures the structure of silica glass is more rigid than at low temperatures. Hence, when arrested in a structural state that corresponds to a high-temperature equilibrium configuration, the room-temperature glass will not only have a higher elastic modulus than the one cooled on an experimental time scale, but upon reheating fewer structural changes can be reverted and the overall increase in elastic modulus will be less.

B. Response to pressure changes

The effect of pressure also reveals anomalous behaviors in our simulated silica glass, matching those observed experimentally. Figure 3 shows the evolution of the bulk modulus under hydrostatic compression at 500 K, 1000 K, and 1500 K. At all temperatures, silica glass exhibits an initial decrease in bulk modulus with pressure until it reaches a minimum at approximately 6 GPa. By applying a hydrostatic tensile stress (negative pressure), the bulk modulus of silica glass continues to increase until pressure reaches −8 GPa. Below −8 GPa and above 6 GPa, silica glass behaves like a

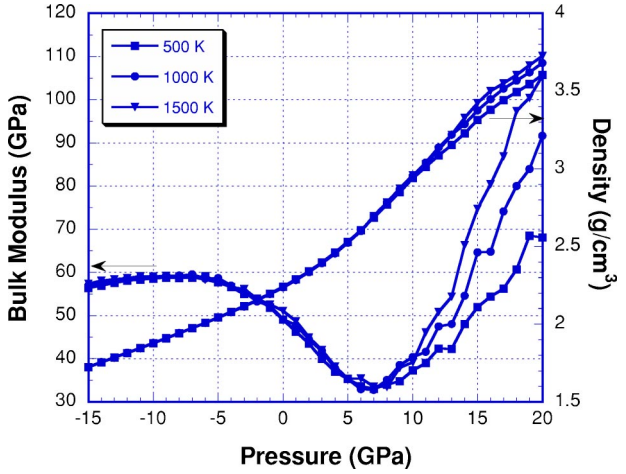

FIG. 3. Density and bulk modulus of silica glass versus pressure at 500 K, 1000 K, and 1500 K from our MD simulations.

normal solid, but in between these pressures, it behaves anomalously. This anomalous behavior of silica glass has long been known from experiments, except for the return to normalcy at large tensile stresses. The bulk modulus of silica glass in our MD simulations exhibits a minimum at a higher pressure than those in most room temperature experiments, where it is found at ~2–3 GPa.[5–9,40] The somewhat higher nadir pressure in our MD simulations, compared to experiments, can again be understood as the result of the high fictive temperatures of the simulated glass. During the rapid quench a portion of the structural relaxation that the simulated glass is capable of is forgone, and compared to experiments, this results in a comparably higher bulk modulus. The structural reorganization that was omitted during the quench must first be completed, now using activation through compressive deformation, before the modulus minimum can be reached. It can be seen in Fig. 3, that the bulk modulus minimum occurs a little bit earlier with increasing temperature, which is consistent with a recent *in situ* study in which the modulus minimum was observed at ~5.7 and 6.7 GPa for 545 and 475 K, respectively.[25] Interestingly, the density of the silica glass in the high-pressure limit increases with increasing temperature, while at ambient pressure in this temperature range silica glass exhibits positive thermal expansion, like a normal solid (see Fig. 1). The negative thermal expansion of silica glass under pressure will be discussed in detail in part II.

C. Structural characteristics

1. Total neutron structure factor

The total neutron structure factor $S(q)$ of the simulated silica glass was calculated from the Fourier transforms of the pair correlation functions. We show the results for different pressures at 500 K in Fig. 4(a). In order not to crowd the graph, we only show $S(q)$ from 1 to 10 GPa. The feature that is predominantly affected by pressure changes is the first sharp diffraction peak (FSDP). It decreases in intensity and shifts towards higher wave-vector magnitude with increasing

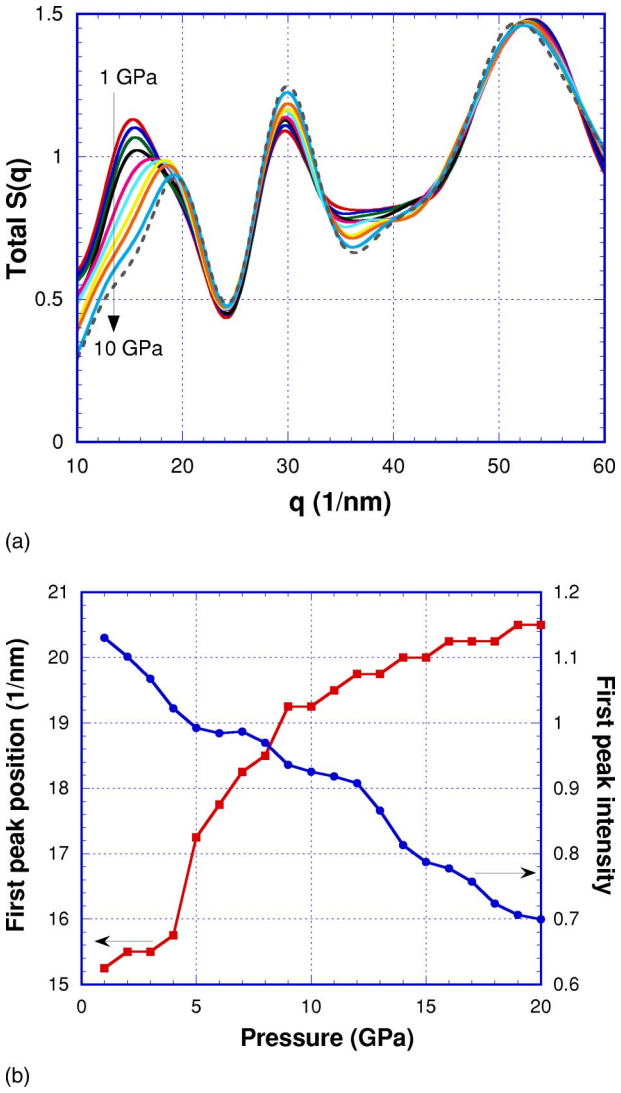

FIG. 4. (a) Total neutron structure factor $S(q)$ of simulated silica glass at 500 K under different pressures. (b) Position and height of the first sharp diffraction peak versus pressure.

pressure, as seen in Fig. 4(b). The second peak remains located at approximately 30 nm^{-1}, but its intensity increases somewhat with pressure. Very little change is observed at larger q. This behavior is in excellent agreement with neutron experiments[16,41] and a molecular-dynamics study.[16] Since features at small q correspond to large repeat distances in real space, the observed changes in the FSDP indicate that the intermediate-range order is substantially more affected by pressure-induced structural modifications than the short-range order.

2. Short range order

Figure 5(a) shows the partial pair-correlation functions $g_{\text{Si-Si}}(r)$, $g_{\text{Si-O}}(r)$, $g_{\text{O-O}}(r)$ of silica glass at pressures of 0, 10, and 20 GPa and at 500 K. Upon densification, the first and second peaks in all pair correlation functions shift to lower distances. The most obvious changes are seen in $g_{\text{Si-Si}}(r)$ distributions, reflecting a reduction of the nearest-neighbor and second-nearest-neighbor Si-Si distances with pressure. Any changes beyond the second peak in $g_{\text{Si-Si}}(r)$, $g_{\text{Si-O}}(r)$, $g_{\text{O-O}}(r)$ are poorly discernable.

The running integrals of the Si-Si, Si-O, and O-O radial distribution functions are plotted for different pressures in Fig. 5(b). At ambient pressure, the coordination numbers derived from plateau levels ($n_{\text{Si-O}}=4$, $n_{\text{O-O}}=6$, $n_{\text{Si-Si}}=4$; $n_{\text{i-j}}$ being the number of species j surrounding species i) are nearly ideal for a continuous random network of corner-sharing SiO_4 tetrahedra. With the increase of pressure from 0 to 20 GPa at 500 K, there is no change in the nearest-neighbor Si-O coordination number, only the gap between the first and the less well defined higher coordination shells narrows.

The O-Si-O and Si-O-Si bond angle distributions are shown in Figs. 5(c) and 5(d). With increasing pressure, the O-Si-O angle distribution still peaks around 109°, however, it shows broadening, indicating slight distortion of the SiO_4 tetrahedra. Most obvious is the change in the intertetrahedral Si-O-Si angle. At 500 K, the peak position shifts continuously from 147° to 135° as the pressure increases from 0 to 20 GPa. The reduction of the Si-O-Si angle, which is consistent with the decrease in the Si-Si nearest-neighbor distance revealed by $g_{\text{Si-Si}}(r)$, has been scrutinized by several researchers,[14,32,42–45] and has been postulated as the mechanism for densification of vitreous silica under pressure.

It has also been proposed that the anomalous increase of the elastic modulus upon heating silica glass,[2] and similarly, the negative thermal expansion of β-cristobalite silica[46,47] is attributed to a reduction in the Si-O-Si angle. While we do observe a slight decrease in the Si-O-Si angle with the increasing temperature in silica glass, the Si-Si distance, in fact, does not decrease. The Si-O-Si angle decreases because the bridging oxygen moves away from the line connecting the two silicon atoms it is bonded to under the influence of thermal energy. All interatomic distances within this triplet of atoms increase with temperature. Thus the Si-O-Si angle reduction cannot be the reason for the elastic anomalies in silica glass.

From the above structural analysis, we see that the SiO_4 tetrahedra maintain their integrity and rigidity at 500 K between 0 and 20 GPa, though they may slightly distort under high pressures. This is in contrast to a recent MD study[24] on the compressibility of pressurized amorphous silica, in which extensive rebonding, leading to Si-O coordination change, is observed at pressures as low as 5 GPa. In experiments, the pressure at which the coordination number of Si changes from 4 to 6 is observed is typically higher, albeit a wide range of magnitudes have been reported. For example, *in situ* high-pressure x-ray diffraction[15] of amorphous SiO_2 shows that the Si coordination starts to surpass 4 at pressures between 8 and 28 GPa and reaches nearly 6 at 42 GPa, while *in situ* Raman[14], infrared,[32] and Brillouin scattering[28] measurements all provide evidence for an increase in Si coordination number only at pressures exceeding 20 GPa. Accordingly, our MD results are in good agreement with experimental observations.

3. Intermediate-range order

The large changes in the FSDP intensity and position of total neutron structure factor, as well as decrease of the Si-

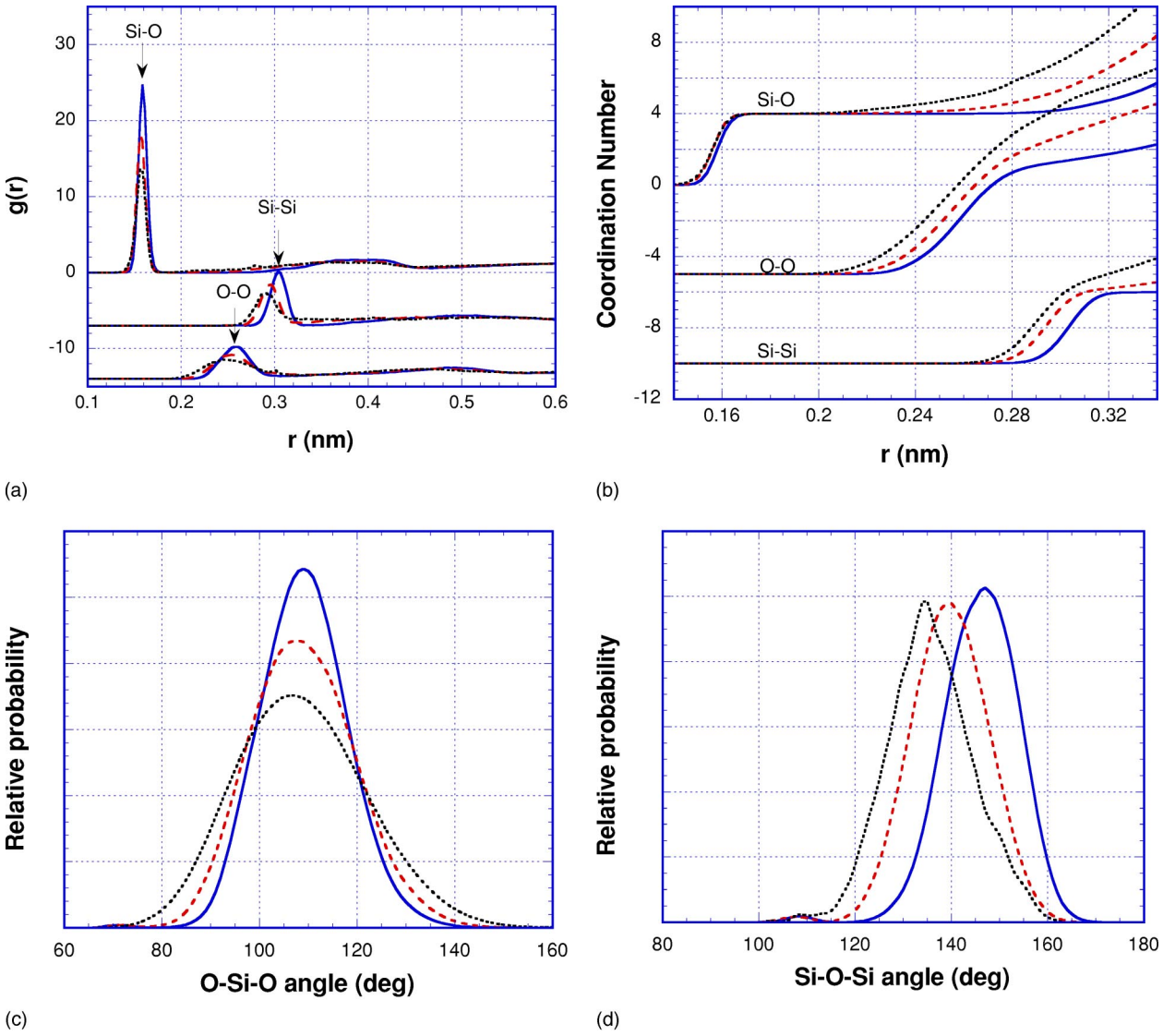

FIG. 5. Short-range order of silica glass at 500 K, 0 GPa (solid line), 10 GPa (dashed line) and 20 GPa (dotted line): (a) radial distribution functions $g_{\text{Si-Si}}(r)$, $g_{\text{Si-O}}(r)$, and $g_{\text{O-O}}(r)$, (b) coordination number, (c) O-Si-O angle distribution, and (d) Si-O-Si angle distribution.

O-Si bond angle with pressure indicate the need for investigating structural features beyond the scale of tetrahedral units. A convenient way to characterize the intermediate-range order of a random network is the ring statistics based on shortest-path analysis.[36–38] The number of Si-O pairs in a ring is conventionally called the size of the ring. Shortest-path analysis ascertains that cristobalite silica consists entirely of six-membered rings, whereas quartz has six- and eight-membered rings.[38,48] The ring size distributions in silica glass as well as the bond lengths and bond angles in these rings have been extensively studied by Rino *et al.*[48] Here we concentrate on changes in ring size distributions along the path of state points that we examined.

At the lowest temperature we studied in our simulations, namely at 500 K, silica glass that has been compressed to 20 GPa recovers its original density upon decompression. This means that the structural transitions in silica glass at 500 K in this pressure range are reversible. The ring statistics of this glass, while subject to pressures that range from 15 GPa to 20 GPa are shown in Fig. 6. Data points for all pressures overlap, and there is no discernible change in the ring size distribution at these pressures. Hence, our MD simulations suggest that densification of silica glass at low temperatures does not involve the breaking or formation of any bonds. This finding concurs with the conclusions drawn by MacMillian *et al.*, who compared the densification of silica glass at high and low temperature.[42] However, our results at high temperatures, which will be discussed in part II of this paper in the context of irreversible changes in the glass structure, show that the average ring size increases with pressure. This is in disagreement with MacMillian *et al.*,[42] who speculated that the densification of silica glass would be consistent with a change to smaller average ring size, but it confirms the results by Stixrude *et al.*,[29] which reveal that the average ring size will increase with pressure if any change happens.

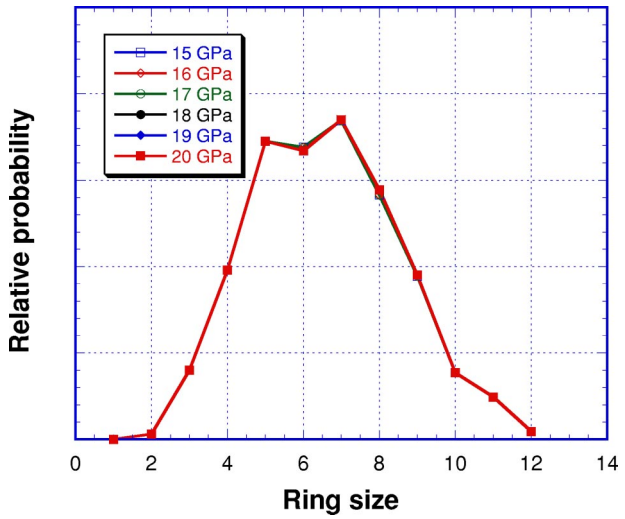

FIG. 6. Ring size distribution at 500 K from 15 to 20 GPa.

It is clear from Fig. 3, that the elastic modulus anomaly under pressure occurs at any of the three temperatures we studied, regardless of whether the ring size changes with pressure or not. For the remainder of part I we will therefore set the effect of thermal activation aside and focus on identifying the structural transitions that are responsible for the anomalous thermomechanical behaviors of silica glass and that apparently do not require the breaking and formation of bonds. We will also ascertain that the underlying mechanism is by nature a transition as opposed to a gradual deformation.

D. Similarities between cristobalite silica and silica glass

By comparing the results in Fig. 2 with those for the anomalous regime between −8 GPa and +6 GPa in Fig. 3, it becomes apparent that, whether it is the result of tensile deformation or thermal expansion, the larger the specific volume of silica glass the higher its bulk modulus. To understand the mechanism responsible for the increase in rigidity as the glass structure expands, we will first reiterate some key findings of our MD simulation study of the phase transformation between the α- and β-cristobalite.[31,49] Given the similarities between cristobalite and silica glass that have been found in the Raman spectra,[50] infrared spectra,[51] Si-O-Si angle distribution,[52] and average ring size,[34] cristobalite has long been a favored archetype for basing structural models of silica glass on. For the following discussion we will introduce two features associated with the α-to-β cristobalite transformation that can also be detected in behavior of silica glass. One pertains to the relationship between volume and elastic property changes upon transformation, the other one to the mechanism by which this transformation takes place.

The first feature is simply stated: while β-cristobalite has the smaller density of the two cristobalite modifications, it has the larger elastic modulus.[53] The sudden changeover from a high-density, low-modulus to a low-density, high-modulus structure upon the pressure-induced α-to-β transformation in simulated cristobalite is shown in Fig. 7(a). β-cristobalite is characterized by more symmetric bond orientations than α-cristobalite [Fig. 7(b)]. In the former, deformation is achieved through bond compression and bending modes that offer equal resistance in all directions, whereas in the latter, due to bond pivoting, rings can twist and fold up onto themselves when compressed.

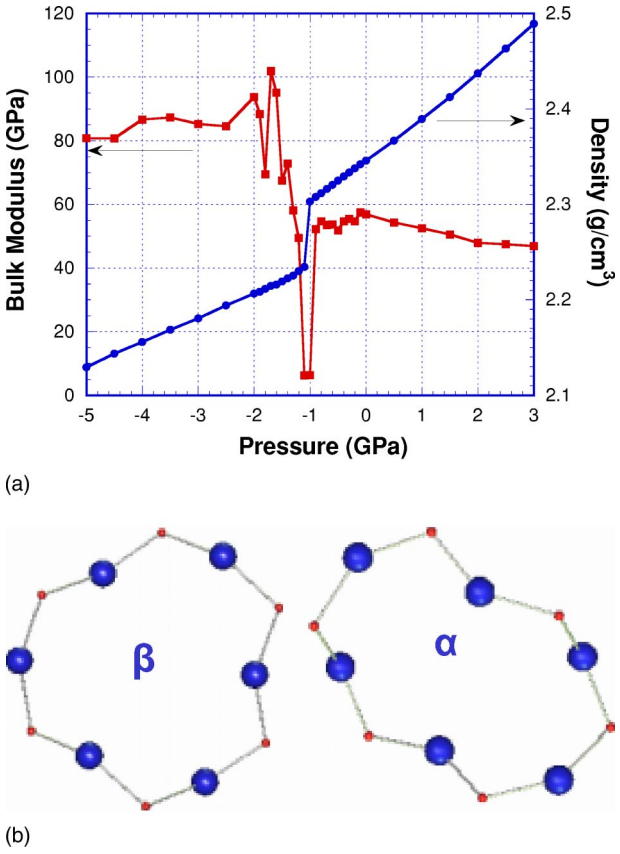

FIG. 7. (a) Density and bulk modulus of cristobalite through the α-to-β transformation under pressure. Main features: α-cristobalite has a higher density, lower symmetry six-membered rings, and lower bulk modulus; β-cristobalite has a lower density, higher symmetry six-membered rings, and higher bulk modulus. (b) Comparison of the geometries of a six-membered ring in α- and β-cristobalite.

As for the second feature, the transition between α- and β-cristobalite is accomplished by a cooperative 90° rotation of Si-O-Si bridges about the Si-Si axis.[31,49] Each atom remains fully bonded to the same nearest neighbors through this transition, and while in the crystal all Si-O-Si bonds rotate simultaneously upon transformation, the process is degenerate in that the rotation can occur in opposite directions within two independent subgroups of bonds. The Si-O-Si bond rotation is so prominent in this process that it can be used to assess the degree of transformation and its spatial extent. We choose as order parameter the normal $\mathbf{n}_i$ to the plane that is defined by the two Si-O bonds connecting a given oxygen,

$$\mathbf{n}_i = \frac{\mathbf{R}_1 \times \mathbf{R}_2}{|\mathbf{R}_1 \times \mathbf{R}_2|}, \tag{1}$$

where $\mathbf{R}_1$ and $\mathbf{R}_2$ are the Si-O vectors in the Si-O-Si plane. The degree of transformation is expressed by comparing in-

stantaneous orientations with that of a reference configuration of known phase character. The temporal evolution of the transformation at any location in the structure can be tracked through the time correlation of an individual Si-O-Si plane normal,

$$C_{n_i}(t) = \mathbf{n}_i(t) \cdot \mathbf{n}_i(0). \quad (2)$$

For a value of $C_{n_i}(t) = 1$, the normal vector $\mathbf{n}_i(t)$has the same orientation as the reference plane normal and no transition has occurred; a value of 0 means the plane has rotated by 90° and the local phase character has changed to a degree equivalent to that of the α-to-β cristobalite transition.

When applying this analysis to silica glass, we find that, in response to temperature or pressure changes, the correlation functions for individual Si-O-Si planes reveal sudden rotations similar to the ones observed during cristobalite transformation. Importantly, the rotations in the glass are abrupt and not gradual. Again, the oxygen atom in the Si-O-Si plane undergoes large displacement while the two Si atoms hardly move. However, unlike in the crystal where rotations of all Si-O-Si bonds are cooperative, in the glass these bonds rotate sporadically and independent from one another. The fraction of bonds affected in this way changes gradually over a range of temperatures or pressures. The effects of pressure and temperature on the structure are, however, not completely analogous. As a function of pressure bond orientations transform between states and remain stable in the new configuration. As seen in Fig. 8(a), two individual planes abruptly rotate at different pressures without thermal activation. A given transition alleviates the local stresses to such an extent that further transitions are not necessary until the stress builds up in a different location as a result of the continued overall compaction. As a function of temperature individual bond configurations are activated to exceed their current energy well and they commence to oscillate between states. In Fig. 8(b), the plane normal correlation function of a given bond is shown at two different temperatures, to point out that on a time average the deviation from the reference orientation (chosen to be that at room temperature) increases with temperature. The mechanical response of the material is determined by the time-averaged bond configurations, which are determinately removed from their initial orientations.

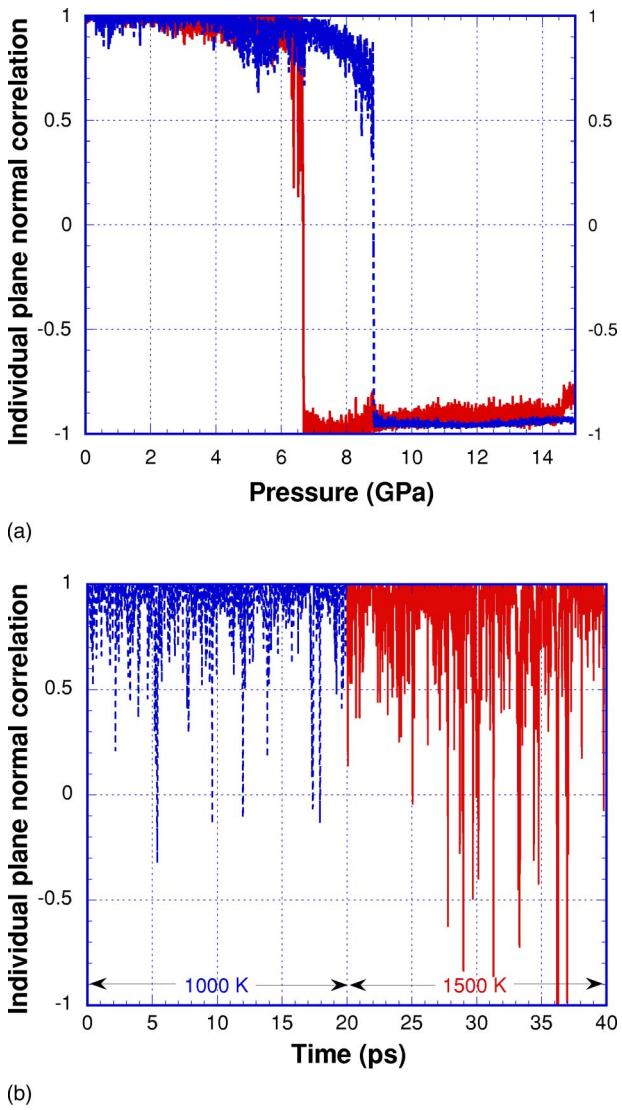

FIG. 8. (a) Two individual plane normal correlation functions versus pressure at 500 K. (b) One individual plane normal correlation function at 1000 K and 1500 K versus time at ambient pressure. (The time origin for data at 1500 K is shifted for clarity.)

E. VDOS and mode instability in silica glass

While the abruptness of Si-O-Si bond rotations is an important indication for these structural changes to be transitions by nature rather than gradual deformations, we want to ascertain this point through further analysis. The underlying idea is that a transition, while it takes place, is characterized by structural instability, whereas deformation is not. This distinction can be made based on a dynamical analysis (DA) of the phase space trajectory of the simulated atomic configuration. A trajectory is considered stable if small perturbations do not affect the system's long-term behavior in any significant way and the phase-space coordinates remain within the potential-energy basin associated with the current configuration. Conversely, if the system is not stable in its current configuration, small perturbations of the phase-space trajectory can grow exponentially and cause the system to escape from its current energy basin.

Determining the rates with which perturbations evolve can therefore be used to assess the stability of a configuration. In principle, there is one such rate for every degree of freedom of the dynamical system, and different numerical procedures for this type of analysis have been suggested in the literature. The square roots of the eigenvalues of the dynamical matrix of the simulated system at any arbitrary point along its trajectory directly yield the complete spectrum of the momentary rates evolution of perturbations.[54,55] This method is computationally similar to normal-mode analysis, except that for the interpretation of the result a subtle but important difference must be made. Because the system is removed from equilibrium and particles are subject to regular acceleration, the eigenvalues of the dynamical matrix do not represent the normal modes of motion of the atoms in the configuration but rather those of a perturbation to their mo-

tion. For an arbitrary configuration of atoms, the resulting eigenvalues may be positive or negative, their square roots real or imaginary, and hence, the temporal evolution of the perturbations to the system may be either monotonous or oscillatory.

In terms of the stability of the system, perturbations that result in oscillatory changes in atomic positions are harmless; it is the perturbations that cause continuously growing deviations from the current trajectory that indicate a propensity of the system to undergo a transition. We refer to the latter as unstable modes. The spectra of eigenvalues for the simulated silica glass are shown in Fig. 9(a). We plot the rates corresponding to the unstable modes on the left-hand side of the origin, with increasing magnitude towards the left, and the rates of oscillatory perturbations on the right-hand side, with increasing magnitude towards the right.[56] The spectrum of oscillatory rates is very closely related to the VDOS of the silica structure. Comparing the VDOS of silica glass from our MD simulations with those from experiments,[57,58] an excellent agreement in the peak position for all three bands (around 400, 800, and 1100 cm^{-1}) is found. Most importantly, in agreement with experiments, we see more features in the low and intermediate frequencies. Most other models for silica glass only give the high-frequency peak and a broad, relatively featureless spectral band in the intermediate and low frequencies.[21,34,59]

The unstable modes are of most interest to us here. At finite temperatures, a small fraction of modes is unstable as a result of thermal disorder. Figure 9(a) shows the DA spectra before, during, and after the abrupt individual Si-O-Si plane rotation that is shown in Fig. 8(a) to occur between 6 and 7 GPa. No substantial difference is seen between these three spectra. However, if we examine the magnitudes of all eigenvectors associated with the O atom that participates in the abrupt rotation before, during, and after the abrupt rotation, as shown in Figs. 9(b)–9(d), we see a huge increase in the magnitude of the eigenvector of one unstable mode during the abrupt plane rotation. This eigenvector points in the direction in which a perturbation would displace the atom with no restoring force, at a speed given by the rate of the corresponding mode. This unstable mode is the localized equivalent of a soft mode observed in displacive transformations of crystals. To our knowledge this occurrence has never before been evidenced in amorphous structures.

To ascertain whether the unstable mode is localized or extended, we can evaluate the participation ratio of the mode using the definition

$$p_\lambda = \left[N \sum_{i=1}^{N} (\mathbf{e}_i^\lambda \cdot \mathbf{e}_i^\lambda)^2 \right]^{-1}, \tag{3}$$

where i runs over N atoms in the system and λ labels the modes.[60] For extended modes p_λ is of the order of unity, while for localized or quasilocalized modes, it will scale inversely with the system size. The participation ratio for modes yielded by our DA during the abrupt rotation is plotted in Fig. 9(e). The participation ratios for the oscillatory modes are in good agreement with the normal mode analysis on vitreous silica by Taraskin and Elliott[61] The participation ratio for the aforementioned unstable mode during the abrupt plane rotation is very low, which means this unstable mode is localized. The molecular structure shown in Fig. 9(f) corresponds to the region in which this mode is localized, cut out from the continuous glass network. The unstable mode eigenvectors are drawn to emanate from the atoms. Their relative magnitudes provide direct visualization of the degree of localization; the larger the eigenvector the more the atom partakes in this mode, and vice versa. Accordingly, the largest amplitude perturbation is to be attributed to the oxygen that undergoes the abrupt rotation, and with increasing distance from this atom eigenvector magnitudes rapidly decrease. To preserve the integrity of the silica network, and given the rigidity of SiO_4 tetrahedra, the oxygen atoms of adjacent tetrahedra must rotate cooperatively. Atoms labeled by large eigenvectors line up in chain or stringlike arrangements. However, atoms beyond two or three interatomic spacing from the central oxygen hardly participate in this unstable mode.

Neutron-scattering experiments[58,62,63] and computer simulations[64] have postulated the existence of the localized cooperative motions in amorphous silica without specifying the nature of these motions. Rotational rearrangements of the SiO_4 in silica glass similar to those reported here, were also observed in simulations by Trachenko *et al.*[65] The low-frequency excitations[66] in silica glass and possibly its unusual properties at very low temperatures,[67] such as the heat-capacity scaling with temperature in a linear rather than cubic way, and the approximately quadratic scaling of the thermal conductivity, have been attributed to these coupled rotations of a few SiO_4 in the glass.

F. Mechanisms underlying the anomalous thermomechanical behavior

Based on the observations detailed above we submit the following explanation for the thermomechanical anomalies exhibited by silica glass. Volume changes, either due to a variation of temperature or mechanical constraints, create stresses in the glass network. These are unevenly distributed across the structure as a result of the disorder associated with the amorphous state of matter. The locations that exhibit peak stress intensities are the first to react to the imposed strains. The most effective way to relieve stress in the network structure is by invoking localized transitions based on the same mechanism that underlies the α-to-β transformation in cristobalite, i.e., the abrupt rotation of Si-O-Si bonds. Accordingly, compressive volume changes lead to the collapse of the network rings that are in their geometries closer to those in α-cristobalite, and hence the structure softens. Conversely, upon expansion the reverse process takes place. While individual bonds rotate abruptly, and this process clearly exhibits the characteristics of a transition, due to the fluctuations in the local stress fields, different network bridges are affected at different degrees of volume change. The average Si-O-Si plane normal orientations, and with that the global properties of the glass structure, therefore only change gradually as a function of pressure or temperature, as can be seen in Figs. 10(a) and 10(b). Because the local phase

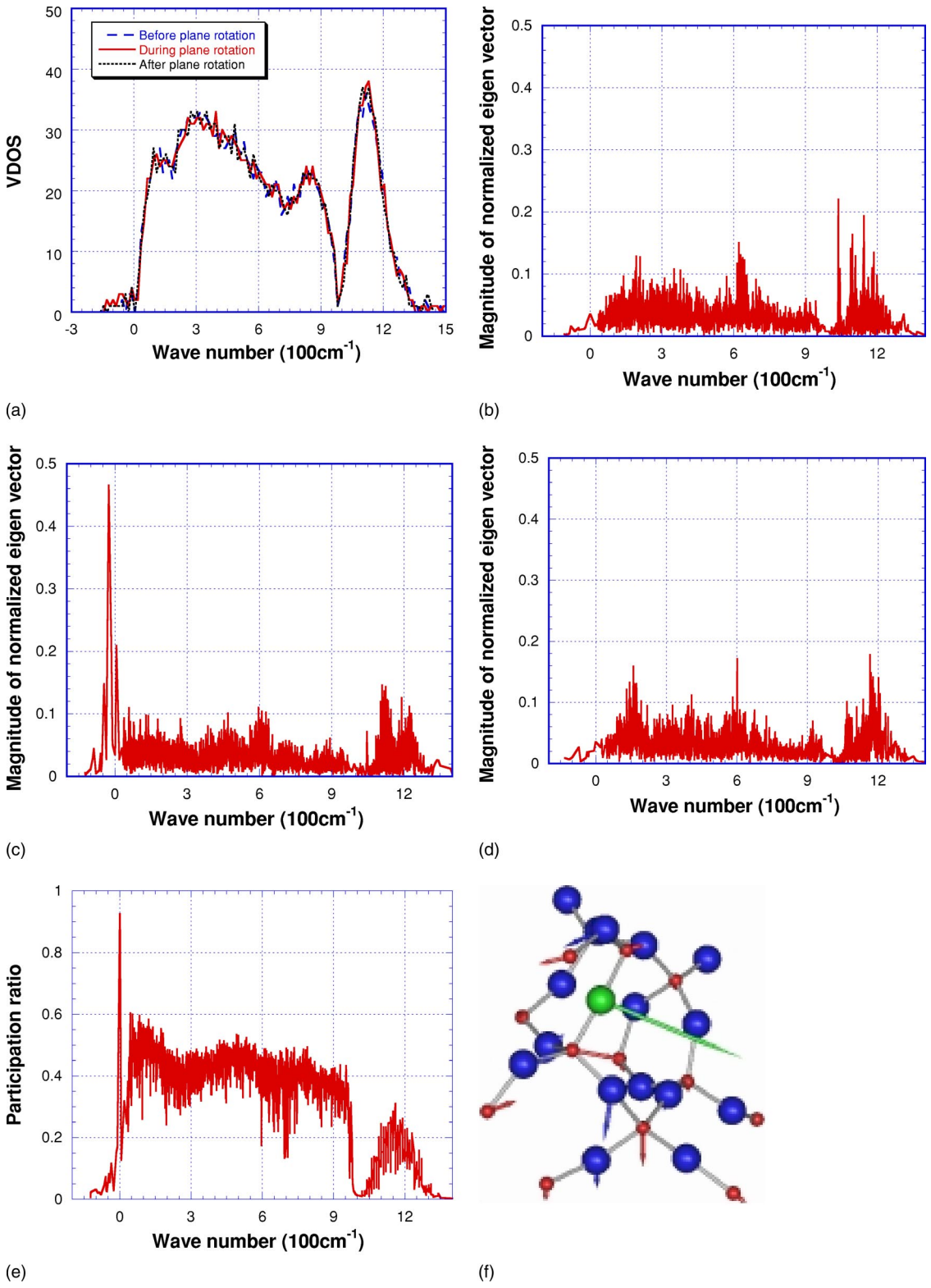

FIG. 9. (a) VDOS before, during, and after the abrupt Si-O-Si plane rotation in silica glass at 500 K (lines overlap to a great extent). Magnitudes of the eigenvectors of all modes describing the effect that a small perturbation has on the trajectory of the O atom involved in a transition, (b) before, (c) during, and (d) after the abrupt plane rotation. (e) Participation ratios of all these modes during the abrupt plane rotation. (f) Structural representation of a group of atoms in the vicinity of the transition: the small spheres represent Si atoms and large ones are O atoms; the large sphere in gray is the O atom undergoing the abrupt rotation. The arrows drawn to emanate from atoms represent the directions and magnitudes of the unstable modes that affect the trajectories of these atoms.

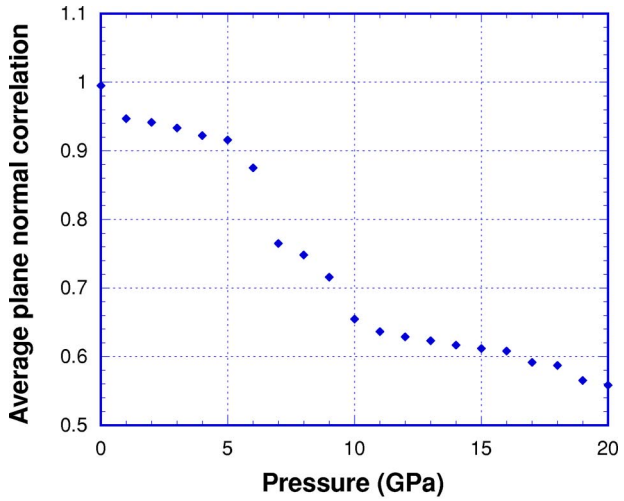

(a)

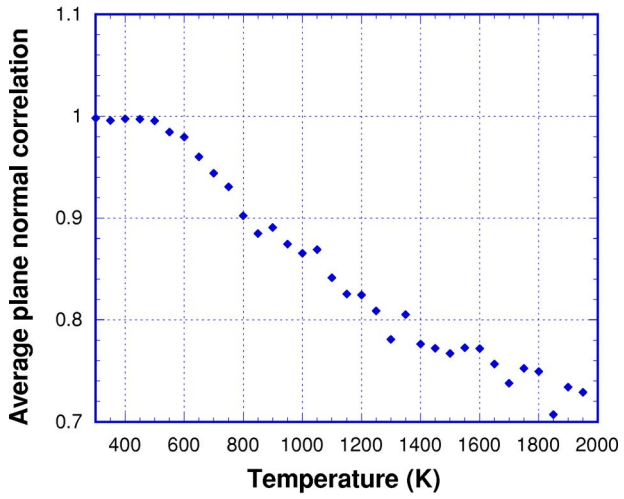

(b)

FIG. 10. Average Si-O-Si plane normal correlation, (a) in silica glass as a function of pressure at 500 K, and (b) in silica glass as a function of temperature at ambient pressure.

character changes from α-like to β-like upon expansion, the bulk modulus of silica glass increases gradually as a result of thermal expansion or tensile deformation. In silica glass, below −8 GPa and above 6 GPa, the ability of the structure to accommodate such transitions saturates and silica glass returns to normal behavior in terms of its mechanical properties.

IV. CONCLUSIONS

To conclude part I, our MD simulations reveal that the thermomechanical anomalies of silica glass are due to the localized reversible structural transitions, which are facilitated by modes of atomic displacement similar to the ones underlying the α-to-β cristobalite phase transformations in crystalline silica, i.e., spontaneous Si-O-Si bond rotations. These transitions take place without changes in the short-range order in the glass structure, i.e., bond length, bond angle, coordination number, and even the ring size distribution remain unaltered. However, the transitions affect the ring geometry and thereby the elastic response of the structure to imposed mechanical constraints. Upon expansion, rings become more symmetric, which eliminates pivoting around Si-O bonds as a mode of deformation. In the expanded structure, all load is borne through bond compression and bond bending, and as a result, the elastic modulus increases. The Si-O-Si bond rotations are associated with dynamical instabilities, which typify this process as polyamorphic transition rather than a gradual deformation, in analogy to soft modes that characterize transformations between crystalline polymorphs. In contrast to displacive transformations in crystals, this polyamorphic transition remains localized, it occurs sporadically at independent locations over a range of pressure or temperature changes and results in a gradual change of phase character and the associated physical properties.

ACKNOWLEDGMENTS

This work was supported by National Institute of Science and Technology, under Grant No. 60NANB9D0102 and the National Science Foundation under Grant No. DMR-0072258. Most of the work is done with NPACI account on AMD clusters in the Center for Advanced Computing (CAC) at University of Michigan. L. Huang would like to thank Dr. X. L. Yuan at MIT for helpful discussion on ring statistics, and Dr. Julian D. Gale at Imperial College of Science, Technology and Medicine, UK for providing GULP codes helping clarifying the dynamical analysis for three-body potential.

*On leave from the Department of Materials Science and Engineering, University of Illinois, Urbana, IL 61801, USA.

[1] J. G. Collins and G. K. White, Prog. Low Temp. Phys. **4**, 450 (1964).
[2] A. Polian, D. Vo-Thanh, and P. Richet, Europhys. Lett. **57**, 375 (2002).
[3] M. Fukuhara and A. Sanpei, Jpn. J. Appl. Phys., Part 1 **33**, 2890 (1994).
[4] R. E. Youngman, J. Kieffer, J. D. Bass, and L. Duffrène, J. Non-Cryst. Solids **222**, 190 (1997).
[5] P. W. Bridgman, Am. J. Sci. **10**, 359 (1925).
[6] P. W. Bridgman, Proc. Am. Acad. Arts Sci. **76**, 9 (1945).
[7] P. W. Bridgman, Proc. Am. Acad. Arts Sci. **76**, 71 (1948).
[8] C. Meade and R. Jeanloz, Phys. Rev. B **35**, 236 (1987).
[9] M. R. Vukevich, J. Non-Cryst. Solids **11**, 25 (1972).
[10] H. M. Cohen and R. Roy, Phys. Chem. Glasses **6**, 149 (1965).
[11] M. Grimsditch, Phys. Rev. Lett. **52**, 2379 (1984).
[12] M. Grimsditch, Phys. Rev. B **34**, 4372 (1986).
[13] M. Grimsditch, R. Bhadra, and Y. Meng, Phys. Rev. B **38**, 7836 (1988).

[14] R. J. Hemley, H. K. Mao, P. M. Bell, and B. O. Mysen, Phys. Rev. Lett. **57**, 747 (1986).
[15] C. Meade, R. J. Hemley, and H. K. Mao, Phys. Rev. Lett. **69**, 1387 (1992).
[16] S. Susman, K. J. Volin, D. L. Price, and M. Grimsditch, Phys. Rev. B **43**, 1194 (1991).
[17] G. D. Mukherjee, S. N. Vaidya, and V. Sugandhi, Phys. Rev. Lett. **87**, 195501 (2001).
[18] C. L. Babcock, S. W. Barder, and K. Fajans, Ind. Eng. Chem. **46**, 161 (1954).
[19] L. V. Woodcock, C. A. Angell, and P. A. Cheeseman, J. Chem. Phys. **65**, 1565 (1976).
[20] J. R. Rustad, D. A. Yuen, and F. J. Spera, Phys. Rev. B **44**, 2108 (1991).
[21] W. Jin, R. K. Kalia, and P. Vashishta, Phys. Rev. Lett. **71**, 3146 (1993).
[22] K. Trachenko and M. T. Dove, J. Phys.: Condens. Matter **14**, 7449 (2002).
[23] K. Trachenko and M. T. Dove, J. Phys.: Condens. Matter **14**, 1143 (2002).
[24] K. Trachenko and M. T. Dove, Phys. Rev. B **67**, 064107 (2003).
[25] F. S. El'kin, V. V. Brazhkin, L. G. Khvostantsev, O. B. Tsiok, and A. G. Lyapin, JETP Lett. **75**, 342 (2002).
[26] R. J. D. Valle and E. Venuti, Phys. Rev. B **54**, 3809 (1996).
[27] J. S. Tse, D. D. Klug, and Y. Le Page, Phys. Rev. B **46**, 5933 (1992).
[28] C. S. Zha, R. J. Hemley, H.-k. Mao, T. S. Duffy, and C. Meade, Phys. Rev. B **50**, 13105 (1994).
[29] L. Stixrude and M. S. T. Bukowinski, Phys. Rev. B **44**, 2523 (1991).
[30] A. Polian and M. Grimsditch, Phys. Rev. B **47**, 13979 (1993).
[31] L. P. Huang and J. Kieffer, J. Chem. Phys. **118**, 1487 (2003).
[32] Q. Williams and R. Jeanloz, Science **239**, 902 (1988).
[33] C. W. Gear, *Numerical Initial Value Problems in Ordinary Differential Equations* (Prentice-Hall, Englewood cliffs, NJ, 1971).
[34] K. Vollmayr, W. Kob, and K. Binder, Phys. Rev. B **54**, 15808 (1996).
[35] H. C. Andersen, J. Chem. Phys. **72**, 2384 (1980).
[36] C. S. Marians and L. W. Hobbs, J. Non-Cryst. Solids **106**, 309 (1988).
[37] D. S. Franzblau, Phys. Rev. B **44**, 4925 (1991).
[38] X. L. Yuan and A. N. Cormack, Comput. Mater. Sci. **24**, 343 (2002).
[39] N. S. O. Ekunwe and D. J. Lacks, Phys. Rev. B **66**, 212101 (2002).
[40] O. B. Tsiok, V. V. Brazhkin, A. G. Lyapin, and L. G. Khvostantsev, Phys. Rev. Lett. **80**, 999 (1998).
[41] Y. Inamura, M. Arai, M. Nakamura, T. Otomo, N. Kitamura, S. M. Bennington, A. C. Hannon, and U. Buchenau, J. Non-Cryst. Solids **293-295**, 389 (2001).
[42] P. MacMillan, B. Piriou, and R. Couty, J. Chem. Phys. **81**, 4234 (1984).
[43] R. A. B. Devine and J. Arndt, Phys. Rev. B **35**, 9376 (1987).
[44] R. A. B. Devine and J. Arndt, Phys. Rev. B **39**, 5132 (1989).
[45] R. A. B. Devine, R. Dupree, I. Farnan, and J. J. Capponi, Phys. Rev. B **35**, 2560 (1987).
[46] E. Bourova, S. C. Parker, and P. Richet, Phys. Rev. B **54**, 12052 (2000).
[47] K. Yamahara, K. Okazaki, and K. Kawamura, J. Non-Cryst. Solids **291**, 32 (2001).
[48] J. P. Rino, I. Ebbsjö, R. K. Kalia, A. Nakano, and P. Vashishta, Phys. Rev. B **47**, 3053 (1993).
[49] L. Duffrène and J. Kieffer, J. Phys. Chem. Solids **59**, 1025 (1998).
[50] V. N. Sigaev, E. N. Smelyanskaya, V. G. Plotnichenko, V. V. Koltashev, A. A. Volkov, and P. Pernice, J. Non-Cryst. Solids **248**, 141 (1999).
[51] M. Handke and M. Mozgawa, Vib. Spectrosc. **5**, 75 (1993).
[52] D. A. Keen and M. T. Dove, J. Phys.: Condens. Matter **11**, 9263 (1999).
[53] Y.-m. Chiang, D. P. Birnie, III, and W. D. Kingery, *Physical Ceramics* (Wiley, New York, 1997).
[54] E. Ott, *Chaos in Dynamical Systems* (Cambridge University Press, Cambridge, 1993).
[55] P. Gaspard, *Chaos, Scattering and Statistical Mechanics* (Cambridge University Press, Cambridge, 1998).
[56] This follows the convention introduced by Keyes *et al.* in the context of their exploration of unstable modes in supercooled and normal liquids [T. Keyes, J. Chem. Phys. **103**, 9810 (1995)].
[57] F. L. Galeener, Phys. Rev. B **27**, 1052 (1983).
[58] J. M. Carpenter and D. L. Price, Phys. Rev. Lett. **54**, 441 (1985).
[59] R. J. D. Valle and E. Venuti, Chem. Phys. **179**, 411 (1994).
[60] S. D. Bembenek and B. B. Laird, J. Chem. Phys. **114**, 2340 (2001).
[61] S. N. Taraskin and S. R. Elliott, Phys. Rev. B **59**, 8572 (1999).
[62] U. Buchenau, N. Nucker, and A. J. Dianoux, Phys. Rev. Lett. **53**, 2316 (1984).
[63] U. Buchenau, H. M. Zhou, N. Nucker, K. S. Gilroy, and W. A. Phillips, Phys. Rev. Lett. **60**, 1318 (1988).
[64] L. Guttman and S. M. Rahman, Phys. Rev. B **33**, 1506 (1986).
[65] K. Trachenko, M. T. Dove, K. D. Hammonds, M. J. Harris, and V. Heine, Phys. Rev. Lett. **81**, 3431 (1998).
[66] M. P. Zaitlin and A. C. Anderson, Phys. Rev. B **12**, 4475 (1975).
[67] R. C. Zeller and R. O. Pohl, Phys. Rev. B **4**, 2029 (1971).